

# 4-oxo-2-thioxo-1,2,3,4-tetrahydropyrimidine-5-carbohydrazide (TC) based materials; DFT, NBO analysis, Fukui function analysis, photovoltaic and solar

Mahmoud Sakr (✉ [Mahmoud.sakr@must.edu.eg](mailto:Mahmoud.sakr@must.edu.eg))

Misr University for Science and Technology

Farag Sherbiny

Al-Azhar University

Abd-Allah El-Etrawy

Misr University for Science and Technology

---

## Research Article

**Keywords:** Solar cells (SCs), Dye-sensitized solar cells (DSSCs), 4-oxo-2-thioxo-1,2,3,4-tetrahydropyrimidine-5-carbohydrazide (TC), Density functional theory (DFT), Natural bond orbital (NBO)

**Posted Date:** March 8th, 2022

**DOI:** <https://doi.org/10.21203/rs.3.rs-1403923/v1>

**License:** © ⓘ This work is licensed under a Creative Commons Attribution 4.0 International License.

[Read Full License](#)

---

# **4-oxo-2-thioxo-1,2,3,4-tetrahydropyrimidine-5-carbohydrazide (TC) based materials; DFT, NBO analysis, Fukui function analysis, photovoltaic and solar cell applications.**

Mahmoud A. S. Sakr<sup>a\*</sup>, Farag F. Sherbiny<sup>c</sup>, Abd-Allah Sh. El-Etrawy<sup>a and b</sup>

<sup>a</sup> *Department of Chemistry, Center of Basic Science (CBS), Misr University for Science and Technology (MUST), Al-Motamayez District, 6th of the October City 77, Egypt.*

<sup>b</sup> *Pharmaceutical Organic Chemistry College of Pharmaceutical Science & Drug Manufacturing, Misr University for Science and Technology (MUST), Al-Motamayez District, 6th of the October City 77, Egypt.*

<sup>c</sup> *Pharmaceutical Organic Chemistry Department, Faculty of Pharmacy (Boys), Al-Azhar University, Cairo 11884, Egypt*

## **• Corresponding author.**

E-mail address: [mahmoud.sakr@must.edu.eg](mailto:mahmoud.sakr@must.edu.eg) (Mahmoud A. S. Sakr) and [abdallah.etrawy@must.edu.eg](mailto:abdallah.etrawy@must.edu.eg) (A. Sh. El-Etrawy).

**Abstract:** Due to numerous pharmaceutical and biological activities 4-oxo-2-thioxo-1,2,3,4-tetrahydropyrimidine-5-carbohydrazide (TC) based materials, it was important to investigate Density functional theory (DFT) calculations, natural bond orbital (NBO) analysis, molecular electrostatic potential (MESP), and local reactivity usage Fukui function for six TC derivatives compounds. DFT, NBO, MESP, and local reactivity calculations were obtained via utilizing CAM-Becke's three-parameter functional and Lee Yange Parr (CAM-B3LYP) functional and 6-311G++(2d, 2p) basis set. Optimized molecular structures for all studied compounds were obtained usage the DFT/CAM-B3LYP/6-311G++(2d, 2p) method. In addition, the highest occupied molecular orbital (HOMO), lowest unoccupied molecular orbital (LUMO), energy gap ( $E_g$ ), light harvest efficiency (LHE), and open-circuit voltage ( $V_{oc}$ ) of all studied MSs are calculated and illustrated. These properties indicate that these molecular modeling structures as good candidates for utilization in organic DSSCs.

**Key words:** Solar cells (SCs); Dye-sensitized solar cells (DSSCs); 4-oxo-2-thioxo-1,2,3,4-tetrahydropyrimidine-5-carbohydrazide (TC); Density functional theory (DFT); Natural bond orbital (NBO).

## 1. Introduction

4-oxo-2-thioxo-1,2,3,4-tetrahydropyrimidine-5-carbohydrazide (TC) based materials are a significant core system and they have gained considerable attention because they are found in various natural and synthetic biologically as well as pharmacologically active compounds [1] due to containing an azomethine moiety (-NH-N = CH-). TC based materials have been reported to possess a broad spectrum of biological activities including, anticancer [2], antithrombotic activity [2], antiviral [3], anticonvulsant [4], analgesic [5], anti-inflammatory [6], antiplatelet [9], antifungal [7], and antimalarial activities [8].

Because of the great challenge used in new research on renewable energy sources, solar cells (SCs) are considered one of the most significant renewable energies recently [9–12]. Photovoltaic (PV) technologies have become one of the most important topics in SCs to convert the sun into electrical energy [13,14]. In addition, the most important challenges represented in capturing solar energy and converting it into electrical energy at a low cost [15]. It was taken out of the PV devices that are based on inorganic materials in their manufacture, such as crystalline and amorphous silicon (Amorph. Si), cadmium telluride (CdTe), gallium arsenide (GaAs), with the knowledge that they give their efficiency from 10 to 32% [16]. However, since these are expensive materials and scarce, in addition to their toxicity, many researchers have resorted to searching for other new, cheap, and more efficient materials. According to what will be said, SCs based on organic compounds are considered an attractive and appropriate choice due to their flexibility and ease of processing in addition to their low cost, but their efficiency at present time is considered less than those that depend on inorganic

materials [17]. The efficiency obtained from these types of cells is still not marketable, as the most efficient devices are 4 to 5 % [18].

Recently, new organic compounds used in SCs have been studied and developed. Among these materials are the dyes for sensitive solar cells (DSSCs), as they receive great interest among researchers due to their low cost and high efficiency in converting solar energy into electricity [19]. Moreover, the manufacture of their devices is easy. Also, PV cells based on the DSSCs have many advantages, including their compatibility with many supporting materials and production under moderate conditions that make them less expensive compared to other DSSCs [20,21]. The first DSSCs were based on titanium dioxide, which was discovered in 1991, and their efficiency was from 7 to 8 percent [13].

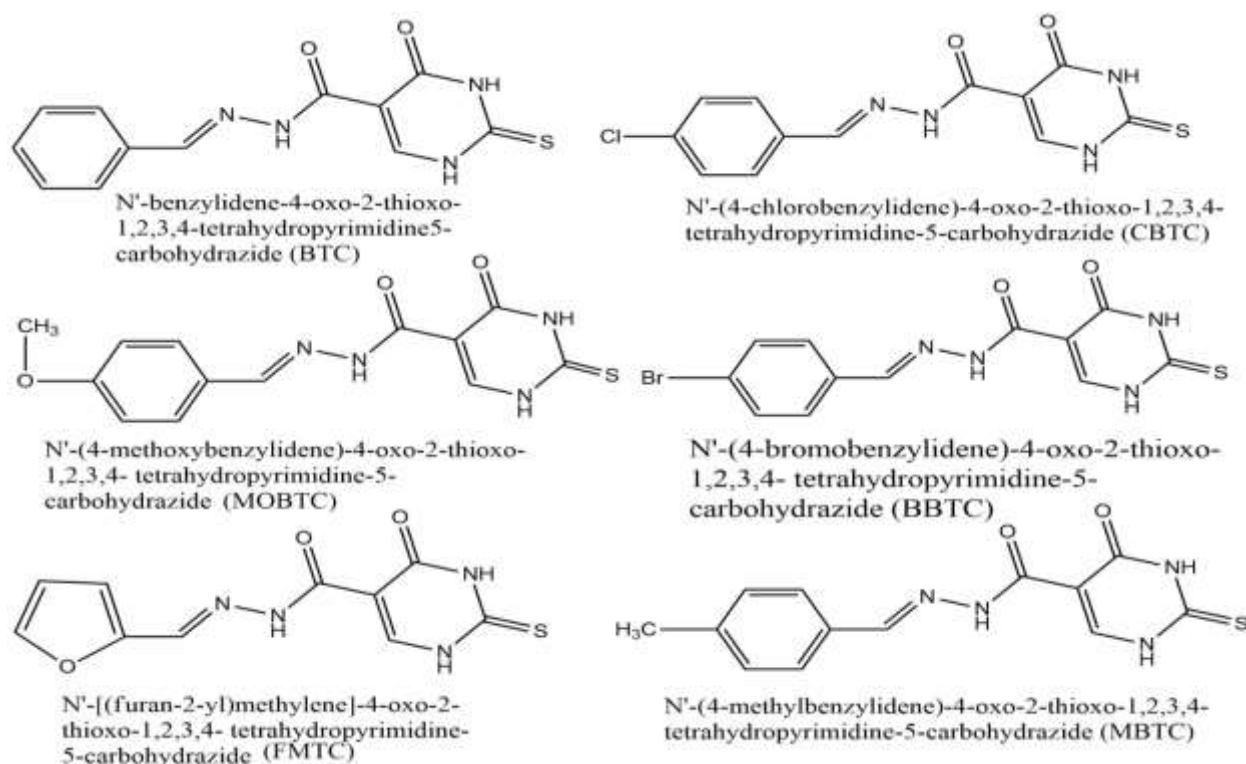
In last the study [22], a series of novel *N'*-(2-thiouracil-5-oyl) hydrazones were designed, chemically synthesized, and characterized [22]. The anticancer results showed that those compounds exhibit the most prominent effect against breast cancer cells [22]. In addition, molecular docking studies were also performed [22]. Hence, it was important to carry out the following important quantum studies in this manuscript; DFT calculations, NBO analysis, Fukui function analysis, MESP, and solar cell application using CAM-B3LYP/6-311G++(2d, 2p) level of theory.

## **2. Studied molecular structures (MSs) and computational investigation**

The molecular modeling and photoelectronic properties of the studied compounds (BTC, CBTC, BBTC, MBTC, MOBTC and FMTC) were investigated using Density functional theory (DFT) methods via utilizing CAM-B3LYP [23] level with 6-311G++(2d, 2p) [24] basis set. All computational calculations were presented via utilizing Gaussian 09 program [24]. Upon utilizing DFT/CAM-B3LYP/6-31G++(2d, 2p) level, the molecular structures (MSs) of neutral molecules are optimized, their molecular electronic properties as HOMO, LUMO

levels and the energy gap ( $E_g$ ) are obtained. The NBO analysis, local reactivity, and electrostatic potential for all studied MSs are calculated via applying DFT/CAM-B3LYP/6-31G++(2d, 2p) level of theory.

All studied MSs(MSs) as shown in Scheme 1 are N'-benzylidene-4-oxo-2-thioxo-1,2,3,4-tetrahydropyrimidine-5-carbohydrazide (BTC), N'-(4-chlorobenzylidene)-4-oxo-2-thioxo-1,2,3,4- tetrahydropyrimidine-5-carbohydrazide (CBTC), N'-(4-methoxybenzylidene)-4-oxo-2-thioxo-1,2,3,4- tetrahydropyrimidine-5-carbohydrazide (MOBTC), N'-(4-bromobenzylidene)-4-oxo-2-thioxo-1,2,3,4- tetrahydropyrimidine-5-carbohydrazide (BBTC), N'-[(furan-2-yl)methylene]-4-oxo-2-thioxo-1,2,3,4- tetrahydropyrimidine-5-carbohydrazide and N'-(4-methylbenzylidene)-4-oxo-2-thioxo-1,2,3,4- tetrahydropyrimidine-5-carbohydrazide (MBTC). The six studied MSs under study were prepared, characterized and published in 2021 [22].



Scheme 1 Studied MSs of BTC, CBTC, BBTC, MBTC, MOBTC and FMTC.

### 3. Result and discussions

#### 3.1 DFT calculations

The optimization of the MSs understudy has been obtained via using DFT/CAM-B3LYP/6-31G++(2d, 2p) method in agaseous state; the results of optimized MSs are presented in Fig. 1. The influence of substituents such as chloride (Cl) in CBTC, bromide (Br) in BBTC, methoxy (CH<sub>3</sub>-O) in MOBTC, methyl (CH<sub>3</sub>-) in MBTC, and furane in FMTC on some important selected optimized MS parameters such as (bond length in Å, bond angle and dihedral angle in degree) for BTC, CBTC, BBTC, MBTC, MOBTC, and FMTC optimized MSs have been investigated; the results are collected in Table 1. Some important comments that can be deduced are as follows; **(i)** Referring to the listed values of dihedral angles, all studied MSs are planar. **(ii)** Owing to increasing bond order, the C<sub>22</sub>-C<sub>20</sub> bond length is less than C<sub>19</sub>-C<sub>17</sub> bond lengths in all Studied MSs by about (0.016-0.088) Å. **(iii)** Referring to the listed values of bond angles, the type of hybridization overall studied MSs is SP<sup>2</sup>. **(iv)** The obtained bond lengths alter because all C-C, ring's C-N bonds are either doubly bonded or partially multiple bonded. **(v)** Generally, the stability of MS can be judged via the length of the bond [25], where the more stable molecular structure is combined by the shorter the bond length. As shown in Table 1, the bond lengths of CBTC, BBTC, MBTC, and MOBTC MSs are less than that of the BTC compound. Therefore, the CBTC, BBTC, MBTC, and MOBTC MSs are the highest stable comparable BTC compound. **(vi)** Also, the bond lengths in FMTC MS are shorter than those in BTC MS. Hence, the FMTC MS is more stable than the BTC compound due to the substitution of furan with the phenyl group.

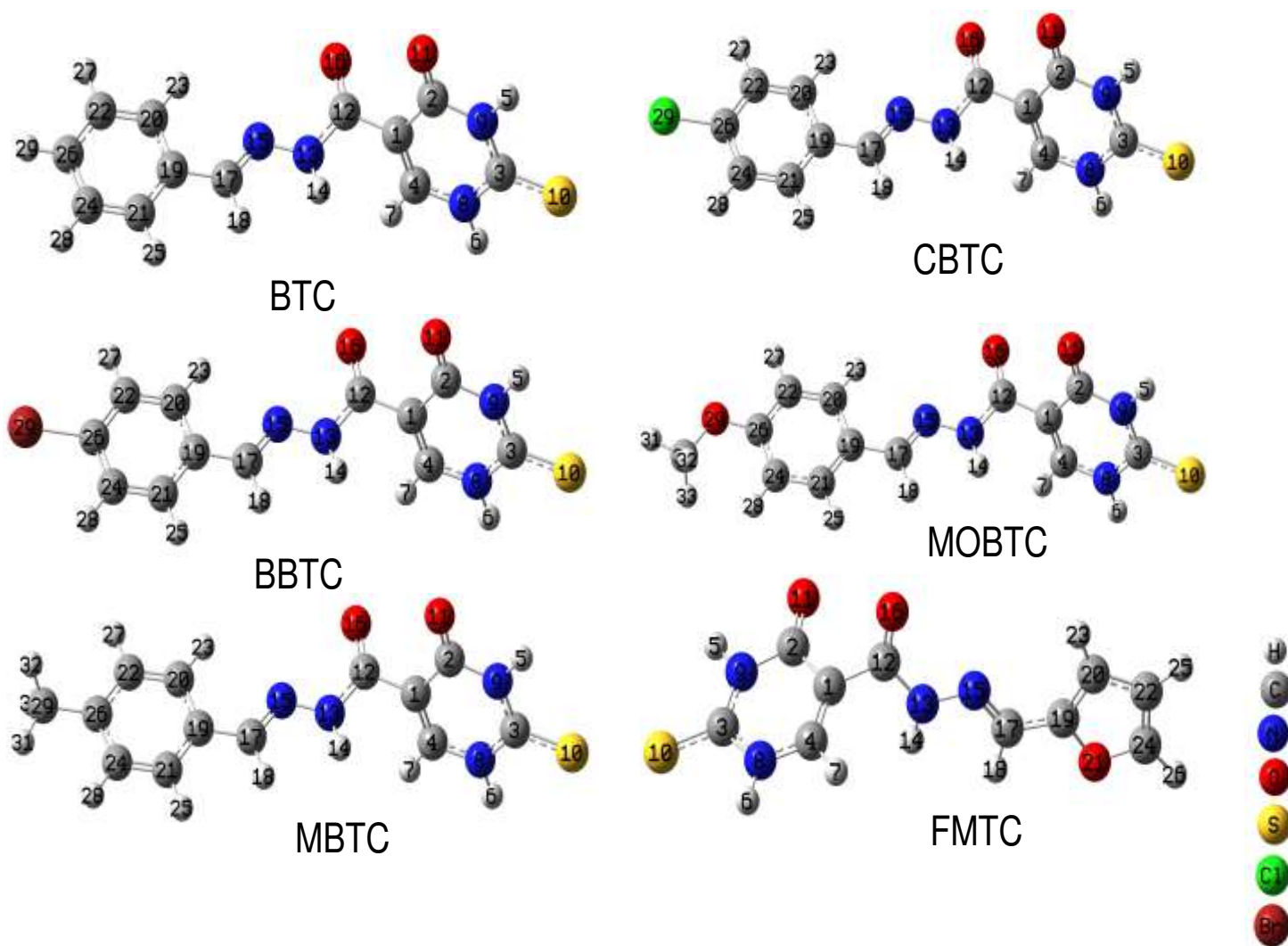


Fig. 1 Optimized MSs of BTC, CBTC, BBTC, MBTC, MOBTC and FMTC in gaseous state using CAM-B3LYP/6-311G++(2d, 2p) level of theory.

Table 1 Selected optimized structural parameters (bond length in °A, bond angle and dihedral angle in degree computed for BTC, CBTC, BBTC, MBTC, MOBTC and FMTC in gaseous phase via applying CAM-B3LYP/6-311G++(2d, 2p) level of theory. For labeling, belong to Fig. 1.

| Designation     | BTC<br>Values | CBTC<br>Values | BBTC<br>Values | MBTC<br>Values | MOBTC<br>Values | FMTC<br>Values |
|-----------------|---------------|----------------|----------------|----------------|-----------------|----------------|
| C22-C20         | 1.380         | 1.378          | 1.378          | 1.376          | 1.370           | 1.379          |
| C19-C17         | 1.463         | 1.462          | 1.462          | 1.460          | 1.458           | 1.438          |
| N15-N13         | 1.360         | 1.354          | 1.354          | 1.357          | 1.359           | 1.358          |
| C12-O16         | 1.209         | 1.197          | 1.197          | 1.198          | 1.198           | 1.203          |
| C2-O11          | 1.207         | 1.200          | 1.200          | 1.200          | 1.201           | 1.206          |
| C3-S10          | 1.666         | 1.651          | 1.651          | 1.652          | 1.652           | 1.660          |
| C22-C20-C19     | 120.16        | 120.44         | 120.44         | 120.16         | 120.54          | 106.36         |
| C17-N15-N13     | 116.73        | 117.58         | 117.58         | 117.23         | 117.11          | 116.87         |
| N9-C3-N8        | 114.24        | 113.6          | 113.6          | 113.61         | 113.62          | 113.31         |
| C22-C20-C19-C17 | 179.98        | 179.99         | 179.93         | 179.97         | 179.97          | 179.79         |
| C19-C17-N15-N13 | 179.67        | 179.39         | 179.35         | 179.37         | 179.35          | 179.51         |
| C12-C1-C4-N8    | 175.82        | 174.03         | 174.03         | 174.01         | 174.01          | 173.7          |

The molecular orbitals (MOs) of all studied MSs (BTC, CBTC, BBTC, MBTC, MOBTC, and FMTC) are investigated; the obtained results such as HOMO (H) / LUMO (L), H-1/L+1, H-2/L+2 MOs, and energy gaps between the following graphically; H and L ( $E_g$ ), H-1 and L+1 ( $E_{g1}$ ) and H-2 and L+2 ( $E_{g2}$ ) in the gaseous state via utilizing CAM-B3LYP/6-311G++(2d, 2p) level of theory are collected in Figs. 2 and 3. The HOMO MOs are localized on phenyl (-C<sub>6</sub>-H<sub>5</sub>) and its derivatives like (4-Cl-C<sub>6</sub>-H<sub>5</sub>, 4-Br-C<sub>6</sub>-H<sub>5</sub>, 4-CH<sub>3</sub>-C<sub>6</sub>-H<sub>5</sub>, and 4-CH<sub>3</sub>-O-C<sub>6</sub>-H<sub>5</sub>) in CBTC, BBTC, MBTC, and MOBTC MSs respectively. But, upon substitution of the phenyl group with furan, the HOMO MOs become localized on furan substituent instead of phenyl one. On the other hand, the LUMO MOs are localized over the whole studied MSs. The HOMO energy MOs of all studied MSs are ordered as follow; BBTC < BTC < CBTC < MBTC < MOBTC < FMTC. Indicating, the BBTC MS has the highest stable HOMO MOs while FMTC MS has

the highest reactive HOMO MOs. Also, the LUMO energy MOs are arranged in the following order: FMTC < BBTC < CBTC < BTC < MBTC < MOBTC. This refers to the FMTC MS having the highest stable LUMO MOs, but the MOBTC has the highest reactive LUMO MOs. The energy gap ( $E_g$ ) value is calculated by applying the difference ( $E_L - E_H$ ). The calculated  $E_g$  values for all studied MSs rise in the following order: FMTC < MOBTC < MBTC < BBTC < CBTC < BTC. These results indicate that the FMTC MS is more reactive comparable to the other studied MSs and BTC has the lowest reactivity. Also, the reduction in the  $E_g$  value favors the red-shifted of the electronic absorption maximum peak in the UV-Vis absorption spectrum. Therefore, the calculated electronic UV-Vis absorption spectra for FMTC, MOBTC, MBTC, BBTC, and CBTC are red shifted, in contrast, UV-Vis absorption spectrum of BTC. The total density of states (TDOS) for BTC, CBTC, BBTC, MBTC, MOBTC, and FMTC MSs using B3LYP/6-31G\* level of theory are investigated; the obtained calculated spectra are collected in Fig. 4. The obtained TDOS for all studied MSs are calculated using Multiwfn software [26]. As presented in Fig. 4, the highest reactive MS is FMTC and the lowest one is BTC.

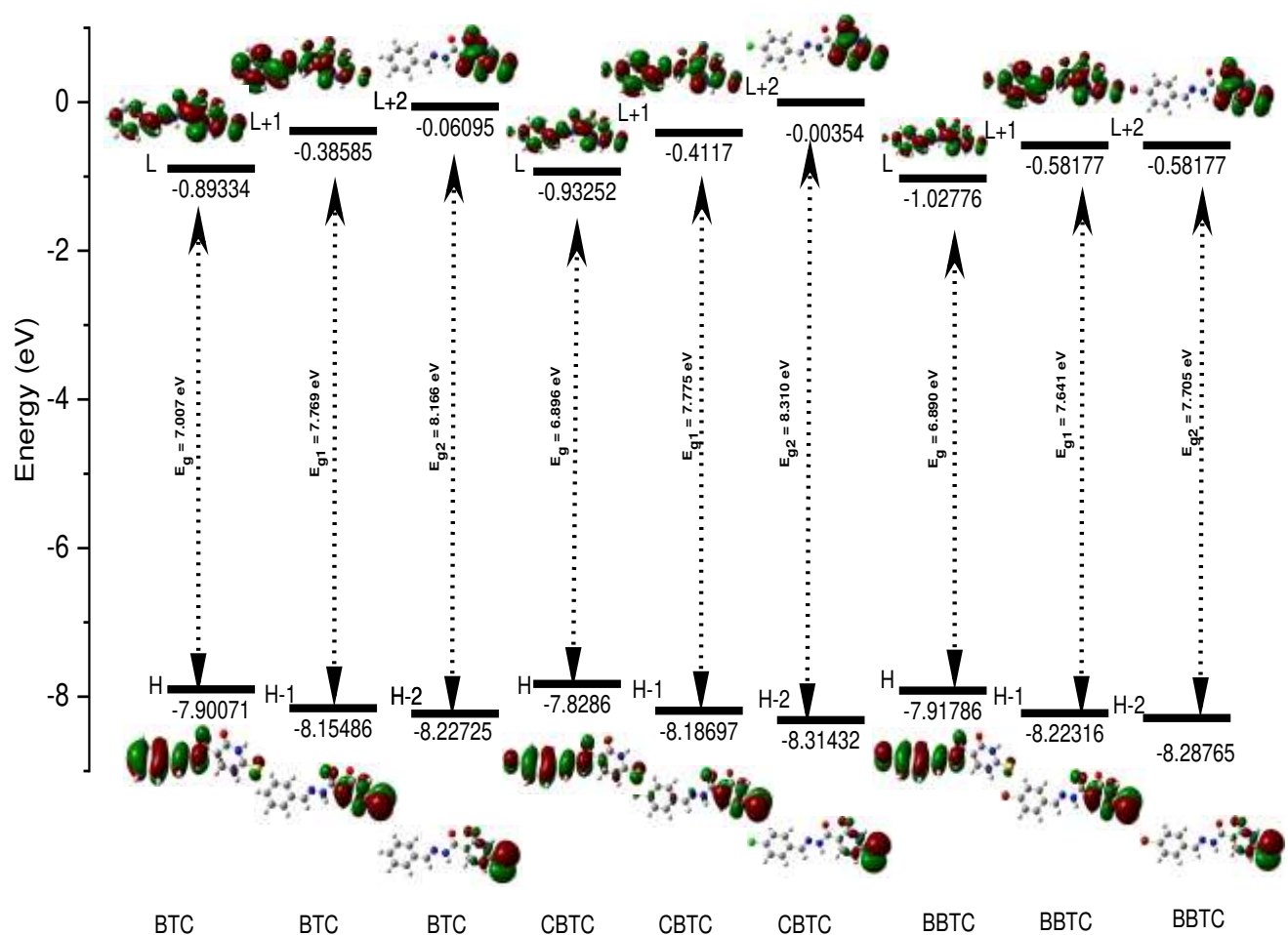


Fig. 2 BTC, CBTC and BBTC molecular modeling graphical presentation of HOMO (H), LUMO (L), H-1, L+1, H-2 and L+2 orbitals as well as energy gaps between the following; H/L ( $E_g$ ), H-1/L+1 ( $E_{g1}$ ) and H-2/L+2 ( $E_{g2}$ ) in gaseous state via utilizing CAM-B3LYP/6-311G++(2d, 2p) level of theory.

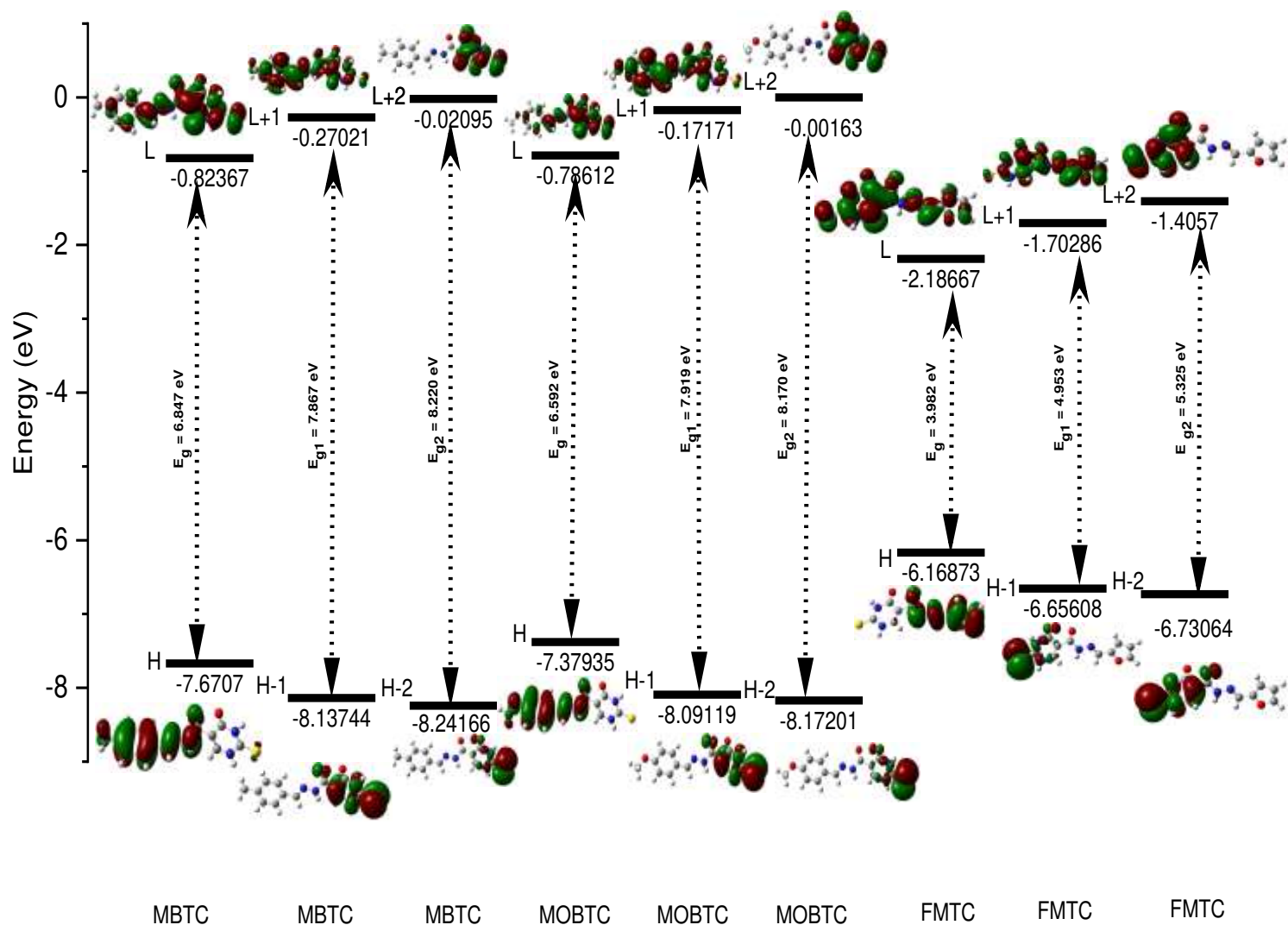


Fig. 3 MBTC, MOBTC and FMTC molecular modeling graphical presentation of HOMO (H), LUMO (L), H-1, L+1, H-2 and L+2 orbitals as well as energy gaps between the following; H/L ( $E_g$ ), H-1/L+1 ( $E_{g1}$ ) and H-2/L+2 ( $E_{g2}$ ) in gaseous state via utilizing CAM-B3LYP/6-311G++(2d, 2p) level of theory.

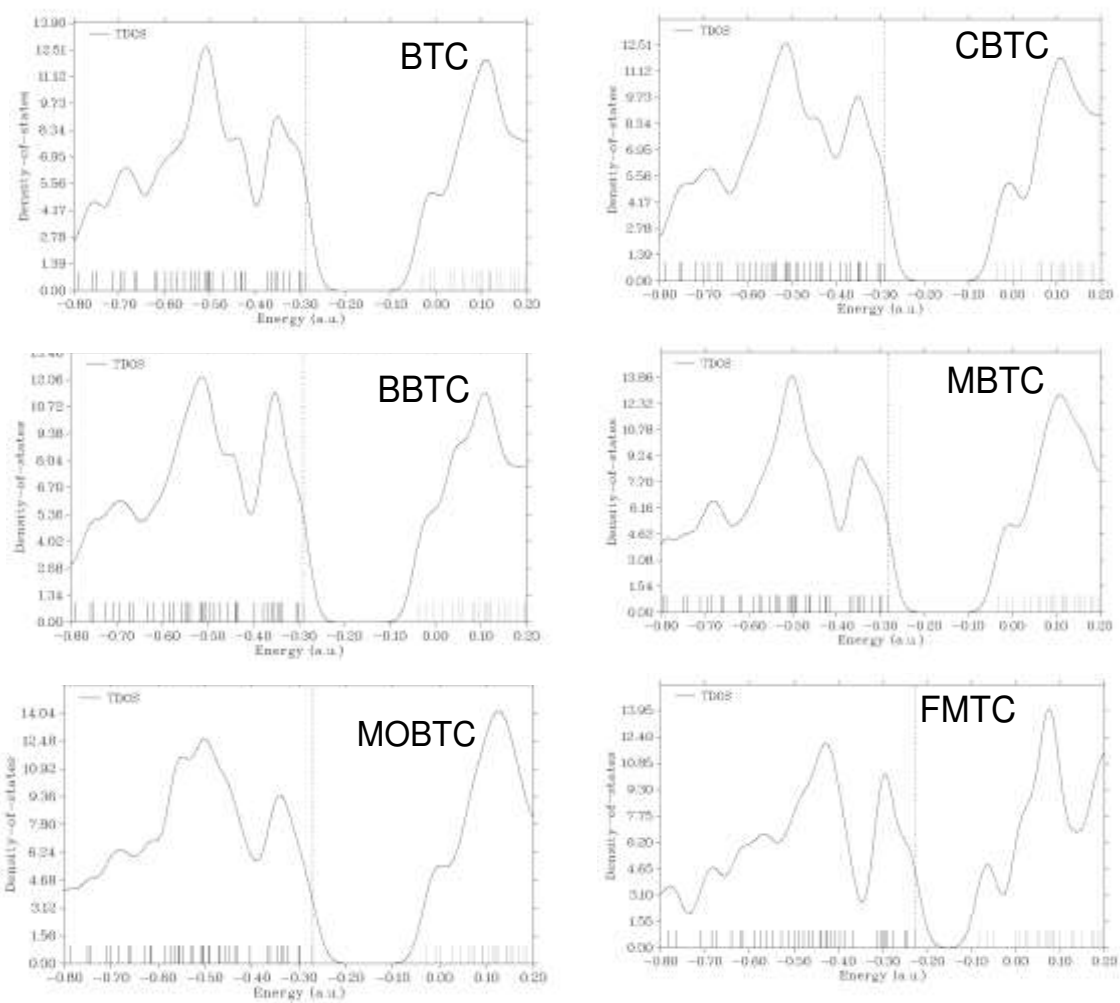


Fig. 4 Total density of states (TDOS) spectra for BTC, CBTC, BBTC, MBTC, MOBTC and FMTC MSs using B3LYP/6-31G\* level of theory.

### 3.2 Quantum chemical parameters calculations

Some important quantum chemical parameters like dipole moment ( $\mu$ ), chemical potential ( $\rho$ ), electronegativity ( $\chi$ ) and chemical hardness ( $\eta$ ) were calculated via using  $E_L$  and  $E_H$  values. These quantum parameters are calculated using the following equations  $\rho = \frac{E_H + E_L}{2}$  [27],  $\chi = -\frac{E_H + E_L}{2}$  and  $\eta = \frac{E_L - E_H}{2}$  [27]. Generally, when the chemical structure has high dipole moment, it has a large asymmetry in the electric charge distribution, and then it can be highly sensitive due to the change of chemical structure and electronic properties under an external electric field. Thus, as shown in Table 2, the  $\mu$  value of the compound BTC is highest in contrasting the rest of the other compounds under study. Therefore, this compound is more active compared to the rest of the compounds under study. As presented in Table 2, the  $\rho$  value of BBTC MS is lower compared to the other studied compounds. Indicating, the escaping electrons from BBTC MS are low comparable to the rest of MSs under study. Also, the high  $\chi$  value for BBTC MS contrasting the other studied MSs (see Table 2) leads to the ability of this compound attracting electrons from other compounds [28]. In another side, the  $\eta$  value for BTC MS is high compared to the rest of the other compounds (see Table 2). This indicates that the BTC compound is exceedingly difficult to liberate electrons, while the other compounds (CBTC, BBTC, MBTC, MOBTC, and FMTC) are good candidates to give electrons to another acceptor molecule.

Table 2 Calculated  $E_H$ ,  $E_L$ , energy gap ( $E_g$ ), dipole moment ( $\mu$ ) and other quantum chemical parameters as electronegativity ( $\chi$ ), chemical potential ( $\rho$ ), chemical hardness ( $\eta$ ) of the BTC, CBTC, BBTC, MBTC, MOBTC and FMTC MSs in gaseous obtained by CAM-B3LYP/6-311G++(2d, 2p) level of theory.

| MSs   | $E_H$ (eV) | $E_L$ (eV) | $E_g$ (eV) | $\mu$ (D) | $\chi$ (eV) | $\rho$ (eV) | $\eta$ (eV) |
|-------|------------|------------|------------|-----------|-------------|-------------|-------------|
| BTC   | -7.900     | -0.893     | 7.007      | 10.40     | 4.3965      | -4.396      | 3.503       |
| CBTC  | -7.828     | -0.932     | 6.896      | 6.301     | 4.380       | -4.380      | 3.448       |
| BBTC  | -7.917     | -1.027     | 6.890      | 6.301     | 4.472       | -4.472      | 3.445       |
| MBTC  | -7.670     | -0.823     | 6.847      | 7.182     | 4.246       | -4.246      | 3.423       |
| MOBTC | -7.379     | -0.786     | 6.593      | 8.489     | 4.082       | -4.082      | 3.296       |
| FMTC  | -6.168     | -2.186     | 3.982      | 8.016     | 4.177       | -4.177      | 1.991       |

### 3.3 NBO Analysis

The NBO analysis gives an efficient methodology for investigating inter- and intramolecular bonding as well as gives a convenient basis for investigating charge transfer or conjugative interactions in molecular systems [29]. The second-order perturbation energies (stabilization or interaction energies) ( $E^2$  (Kcal/mol)) and the most significant interaction between Lewis's type NBOs (donor) and non-Lewis NBOs (acceptor) for all studied MSs are calculated using NBO analysis at CAM-B3LYP/6-311G++(2d, 2p) level of theory; the collected data are summarized in Table 3. The results of NBO analysis for BTC, CBTC, BBTC, MBTC, MOBTC, and FMTC MSs indicate that there is a strong hyper conjugative interaction as follow; (1) LP (1) N8  $\rightarrow$   $\pi^*C1-C4$  and  $\pi^*C3-S10$ , LP (1) N9  $\rightarrow$   $\pi^*C2-O11$  and  $\pi^*C3-S10$  as well as LP (1) N13  $\rightarrow$   $\pi^*C12-O16$  and  $\pi^*N15-C17$ , for all studied MSs (the values of stabilized energy are written in Table 3). Due to furan substituent in FMTC MS, the hyper conjugative energies values for FMTC MS are lowest in contrasting the other studied MSs (BTC, CBTC, BBTC, MBTC, and

MOBTC MSs). This indicates the highest reactivity of this compound (FMTC) compared to other studied compounds. As presented in Table 3, the all hyper conjugative interactions values for MBTC and MOBTC are increased compared to BTC MS except  $\pi\text{C19-C21} \rightarrow \pi^*\text{C24-C26}$ ,  $\pi\text{C20-C22} \rightarrow \pi^*\text{C19-C21}$ ,  $\pi\text{C24-C26} \rightarrow \pi^*\text{C20-C22}$ , LP (1) N8  $\rightarrow \pi^*\text{C1-C4}$ , LP (1) N9  $\rightarrow \pi^*\text{C2-O11}$ , LP (1) N13  $\rightarrow \pi^*\text{N15-C17}$  and LP (2) O16  $\rightarrow \pi^*\text{C11-N13}$  hyper conjugative interactions due to electron-donating properties for  $\text{CH}_3$ - and  $\text{CH}_3\text{-O}$ - substituent at the para position of the phenyl group in MBTC and MOBTC MSs respectively. On the other side, the following hyper conjugative interactions for CBTC and BBTC MSs;  $\pi\text{C1-C4} \rightarrow \pi^*\text{C2-O11}$ ,  $\pi\text{C19-C21} \rightarrow \pi^*\text{N15-C17}$ ,  $\pi\text{C20-C22} \rightarrow \pi^*\text{C19-C21}$ ,  $\pi\text{C24-C26} \rightarrow \pi^*\text{C20-C22}$  and  $\pi^*\text{C19-C21}$ , LP (1) N8  $\rightarrow \pi^*\text{C3-S10}$ , LP (1) N9  $\rightarrow \pi^*\text{C2-O11}$  and  $\pi^*\text{C3-S10}$ , LP (2) O11  $\rightarrow \pi^*\text{C2-N9}$ , LP (1) N13  $\rightarrow \pi^*\text{C12-O16}$  and LP (2) O16  $\rightarrow \pi^*\text{C1-C12}$  decreased comparable BTC compound due to electron-withdrawing properties for Cl and Br substituents at the para position of the phenyl group in CBTC and BBTC MSs respectively.

Table 3 Selection of most influential second order perturbation ( $E^2$ ) estimation of the hyper conjugative energies (kcal/mol) of the BTC, CBTC, BBTC, MBTC, MOBTC and FMTC molecular modeling structure which were calculated using CAM-B3LYP/6-311G++(2d, 2p)) level of theory.

| Donor         | Acceptor        | $E^2$ (Kcal/mol) |       |       |       |       |       |
|---------------|-----------------|------------------|-------|-------|-------|-------|-------|
|               |                 | BTC              | CBTC  | BBTC  | MBTC  | MOBTC | FMTC  |
| $\pi$ C1-C4   | $\pi^*$ C2-O11  | 26.78            | 26.73 | 26.73 | 26.81 | 26.83 | 21.67 |
| $\pi$ C19-C21 | $\pi^*$ N15-C17 | 21.58            | 21.15 | 21.07 | 22.42 | 23.79 | 18.79 |
| $\pi$ C19-C21 | $\pi^*$ C20-C22 | 27.16            | 27.81 | 27.61 | 27.36 | 28.45 | 16.79 |
| $\pi$ C19-C21 | $\pi^*$ C24-C26 | 28.73            | 30.85 | 31.09 | 26.65 | 23.64 | -     |
| $\pi$ C20-C22 | $\pi^*$ C19-C21 | 30.36            | 29.11 | 29.47 | 28.46 | 24.71 | -     |
| $\pi$ C20-C22 | $\pi^*$ C24-C26 | 31.32            | 32.39 | 32.36 | 32.04 | 32.1  | -     |
| $\pi$ C24-C26 | $\pi^*$ C20-C22 | 27.60            | 26.21 | 26.52 | 25.7  | 21.46 | -     |
| $\pi$ C24-C26 | $\pi^*$ C19-C21 | 31.61            | 29.04 | 28.59 | 33.62 | 35.01 | -     |
| LP (1) N8     | $\pi^*$ C1-C4   | 49.93            | 50.29 | 50.31 | 49.76 | 49.53 | 40.25 |
| LP (1) N8     | $\pi^*$ C3-S10  | 80.07            | 79.63 | 79.62 | 80.28 | 80.54 | 64.35 |
| LP (1) N9     | $\pi^*$ C2-O11  | 56.02            | 56.14 | 56.13 | 55.97 | 55.92 | 45.14 |
| LP (1) N9     | $\pi^*$ C3-S10  | 94.00            | 93.75 | 93.79 | 94.11 | 94.23 | 75.71 |
| LP (2) O11    | $\pi^*$ C1-C2   | 23.80            | 23.93 | 23.93 | 23.84 | 23.81 | 20.15 |
| LP (2) O11    | $\pi^*$ C2-N9   | 36.64            | 36.62 | 36.62 | 36.65 | 36.66 | 31.09 |
| LP (1) N13    | $\pi^*$ C12-O16 | 49.81            | 49.41 | 49.41 | 49.96 | 50.06 | 40.21 |
| LP (1) N13    | $\pi^*$ N15-C17 | 29.84            | 30.75 | 30.81 | 29.36 | 28.78 | 26.82 |
| LP (2) O16    | $\pi^*$ C1-C12  | 26.33            | 26.23 | 26.23 | 26.36 | 26.41 | 22.18 |
| LP (2) O16    | $\pi^*$ C11-N13 | 35.02            | 35.31 | 35.33 | 34.85 | 34.65 | 29.48 |

### 3.4 Local Reactivity using Fukui function

The local reactivity of all atoms in all studied MSs using Fukui function at the DFT/CAM-B3LYP/6-311G++(2d, 2p) were investigated; the calculated results are written in Tables 4, 5 and 6 [30]. The electrophilic ( $f^-$ ), nucleophilic ( $f^+$ ) and free radical ( $f^0$ ) attack are calculated via utilizing the following equations;  $f^+ = [q(N+1)-q(N)]$ ,  $f^- = [q(N)-q(N-1)]$  and  $f^0 = [q(N+1) - q(N-1)]/2$  where  $q$  is atomic charge (Mulliken, Hirschfeld or NBO, etc.) at the atomic site in the anionic (N+1), cationic (N-1) or neutral molecule (N). For all studied MSs, the order of the reactive sites for the electrophilic attack, nucleophilic attack, and free radical

attacks was collected in Tables 4, 5, and 6. For BTC MS, the parameters of local reactivity descriptors show that 10S is the more reactive site for nucleophilic and free radical attacks and 13N for electrophilic attack due to electron-donating (ED) properties of oxygen atom in carbonyl group and nitrogen atom in azomethine moiety (-NH-N = CH-). For BBTC MS, the most reactive site for nucleophilic, free radical, and electrophilic attack is 26C, 16O, and also 16O respectively due to the ED properties of oxygen atoms in the carbonyl group. For FMTC MS, the most reactive site for nucleophilic, free radical, and electrophilic attack is 10S due to ED effects of the oxygen hetero atom in furan substituent. The highest reactive site of electrophilic attack for CBTC MS is 29Cl and the most reactive site for nucleophilic and free radical attack is 10S due to high electron-withdrawing (EW) properties of chloride substituent. For MOBTC and MBTC MSs, the most reactive electrophilic and nucleophilic attack is the same which is 1C and 10S respectively. But the free radical attack for MOBTC and MBTC MSs is not the same which is 1C for MOBTC and 16O for MBTC. This is due to the highest ED properties for the CH<sub>3</sub>-O group in the MOBTC MS contrasting CH<sub>3</sub>- group in MBTC compound. (Note: All the compounds under study are compared to the BTC compound, and therefore the reasons for the highest reactive site for nucleophilic, free radical and electrophilic attack depend on this comparison).

Table 4 Order of the reactive sites on compounds BTC and BBTC

| BTC   |        |        |        |                |                |                | BBTC   |        |        |        |                |                |                |
|-------|--------|--------|--------|----------------|----------------|----------------|--------|--------|--------|--------|----------------|----------------|----------------|
| Atoms | q(N)   | q(N+1) | q(N-1) | f <sup>-</sup> | f <sup>+</sup> | f <sup>0</sup> | Atoms  | q(N)   | q(N+1) | q(N-1) | f <sup>-</sup> | f <sup>+</sup> | f <sup>0</sup> |
| 1(C)  | -0.046 | -0.112 | -0.056 | 0.01           | 0.0655         | 0.0277         | 1(C)   | 0.0127 | -0.036 | -0.002 | -0.014         | -0.023         | -0.019         |
| 2(C)  | 0.1746 | 0.144  | 0.176  | 0.0014         | 0.03           | 0.0157         | 2(C)   | 0.4201 | 0.4259 | 0.4175 | -0.002         | -0.005         | -0.004         |
| 3(C)  | 0.111  | 0.068  | 0.1124 | 0.0014         | 0.0422         | 0.0218         | 3(C)   | 0.4142 | 0.4455 | 0.3823 | -0.031         | -0.031         | -0.031         |
| 4(C)  | 0.0433 | -0.063 | 0.0549 | 0.0115         | 0.1068         | 0.0592         | 4(C)   | 0.0915 | 0.0875 | 0.1159 | 0.0244         | 0.0041         | 0.0142         |
| 8(N)  | -0.044 | -0.060 | -0.034 | 0.0098         | 0.0156         | 0.0127         | 8(N)   | -0.315 | -0.094 | -0.318 | -0.002         | -0.221         | -0.111         |
| 9(N)  | -0.052 | -0.085 | -0.048 | 0.0041         | 0.0326         | 0.0183         | 9(N)   | -0.298 | -0.282 | -0.300 | -0.001         | -0.016         | -0.009         |
| 10(S) | -0.282 | -0.456 | -0.206 | 0.0761         | 0.1739         | 0.1250         | 10(S)  | -0.284 | -0.587 | -0.237 | 0.0464         | 0.3035         | 0.1749         |
| 11(O) | -0.266 | -0.326 | -0.256 | 0.0101         | 0.0597         | 0.0349         | 11(O)  | -0.377 | -0.421 | -0.372 | 0.0054         | 0.044          | 0.0247         |
| 12(C) | 0.1679 | 0.136  | 0.1931 | 0.0253         | 0.0319         | 0.0286         | 12(C)  | 0.4036 | 0.0033 | 0.3916 | -0.011         | 0.4003         | 0.1942         |
| 13(N) | -0.046 | -0.049 | 0.0448 | 0.0913         | 0.0033         | 0.0473         | 13(N)  | -0.230 | -0.284 | 0.0074 | 0.2380         | 0.0537         | 0.1459         |
| 15(N) | -0.078 | -0.097 | -0.005 | 0.0724         | 0.0197         | 0.0461         | 15(N)  | -0.126 | -0.125 | -0.027 | 0.0981         | -0.000         | 0.0487         |
| 16(O) | -0.264 | -0.322 | -0.188 | 0.0757         | 0.0582         | 0.0670         | 16(O)  | -0.376 | -0.783 | -0.338 | 0.0381         | 0.4075         | 0.2228         |
| 17(C) | 0.027  | -0.028 | 0.0859 | 0.0589         | 0.0551         | 0.057          | 17(C)  | 0.115  | 0.1265 | -0.242 | -0.357         | -0.011         | -0.184         |
| 19(C) | -0.009 | -0.013 | 0.0424 | 0.0518         | 0.0039         | 0.0279         | 19(C)  | -0.009 | 0.0134 | 0.3002 | 0.3092         | -0.022         | 0.1434         |
| 20(C) | -0.028 | -0.045 | 0.0219 | 0.0501         | 0.0173         | 0.0337         | 20(C)  | -0.035 | -0.039 | 0.0407 | 0.0764         | 0.0038         | 0.0401         |
| 21(C) | -0.039 | -0.059 | 0.0118 | 0.0513         | 0.0195         | 0.0354         | 21(C)  | -0.018 | -0.034 | -0.007 | 0.0107         | 0.0161         | 0.0134         |
| 22(C) | -0.034 | -0.051 | 0.0039 | 0.0382         | 0.0171         | 0.0276         | 22(C)  | -0.060 | -0.043 | 0.000  | 0.0602         | -0.017         | 0.0216         |
| 24(C) | -0.039 | -0.059 | 0.0059 | 0.0457         | 0.0191         | 0.0324         | 24(C)  | -0.013 | 0.0311 | -0.028 | -0.015         | -0.044         | -0.029         |
| 26(C) | -0.033 | -0.070 | 0.0579 | 0.0912         | 0.0368         | 0.064          | 26(C)  | 0.0485 | 0.0423 | 0.3654 | 0.3169         | 0.0062         | 0.1615         |
|       |        |        |        |                |                |                | 29(Br) | -0.115 | -0.155 | -0.046 | 0.0694         | 0.0404         | 0.0549         |

Table 5 Order of the reactive sites on compounds CBTC and MOBTC

| CBTC   |        |        |        |                |                |                | MOBTC |        |        |        |                |                |                |
|--------|--------|--------|--------|----------------|----------------|----------------|-------|--------|--------|--------|----------------|----------------|----------------|
| Atoms  | q(N)   | q(N+1) | q(N-1) | f <sup>-</sup> | f <sup>+</sup> | f <sup>0</sup> | Atoms | q(N)   | q(N+1) | q(N-1) | f <sup>-</sup> | f <sup>+</sup> | f <sup>0</sup> |
| 1(C)   | -0.047 | -0.095 | -0.056 | 0.0094         | 0.0479         | 0.0192         | 1(C)  | -0.046 | -0.121 | -0.056 | 0.098          | 0.0751         | 0.327          |
| 2(C)   | 0.1746 | 0.1517 | 0.1759 | 0.0013         | 0.0228         | 0.0121         | 2(C)  | 0.1745 | 0.1404 | 0.1752 | 0.0007         | 0.0341         | 0.0174         |
| 3(C)   | 0.1111 | 0.079  | 0.1123 | 0.0012         | 0.0321         | 0.0166         | 3(C)  | 0.111  | 0.0632 | 0.1115 | 0.0005         | 0.0478         | 0.0242         |
| 4(C)   | 0.0438 | -0.043 | 0.0544 | 0.0106         | 0.0873         | 0.0489         | 4(C)  | 0.0427 | -0.073 | 0.0516 | 0.0089         | 0.1163         | 0.0626         |
| 8(N)   | -0.044 | -0.058 | -0.035 | 0.009          | 0.0136         | 0.0113         | 8(N)  | -0.045 | -0.061 | -0.038 | 0.0066         | 0.0163         | 0.0115         |
| 9(N)   | -0.052 | -0.077 | -0.048 | 0.0037         | 0.025          | 0.0144         | 9(N)  | -0.052 | -0.089 | -0.050 | 0.0028         | 0.0367         | 0.0198         |
| 10(S)  | -0.28  | -0.426 | -0.209 | 0.0706         | 0.1466         | 0.1086         | 10(S) | -0.285 | -0.473 | -0.227 | 0.0577         | 0.1873         | 0.1225         |
| 11(O)  | -0.266 | -0.313 | -0.257 | 0.0091         | 0.0469         | 0.028          | 11(O) | -0.267 | -0.333 | -0.260 | 0.0065         | 0.0666         | 0.0365         |
| 12(C)  | 0.1687 | 0.1321 | 0.1918 | 0.0231         | 0.0367         | 0.0299         | 12(C) | 0.1663 | 0.1387 | 0.1878 | 0.0215         | 0.0276         | 0.0245         |
| 13(N)  | -0.045 | -0.050 | 0.0364 | 0.0824         | 0.0047         | 0.0435         | 13(N) | -0.048 | -0.050 | 0.0146 | 0.0627         | 0.0027         | 0.0327         |
| 15(N)  | -0.076 | -0.113 | -0.008 | 0.068          | 0.0372         | 0.0526         | 15(N) | -0.085 | -0.094 | -0.014 | 0.0705         | 0.0088         | 0.0396         |
| 16(O)  | -0.262 | -0.322 | -0.194 | 0.0679         | 0.06           | 0.064          | 16(O) | -0.267 | -0.322 | -0.209 | 0.0579         | 0.0551         | 0.0565         |
| 17(C)  | 0.0262 | -0.039 | 0.0765 | 0.0503         | 0.066          | 0.0581         | 17(C) | 0.0256 | -0.021 | 0.0565 | 0.0308         | 0.0475         | 0.0392         |
| 19(C)  | -0.008 | -0.019 | 0.0445 | 0.0531         | 0.0109         | 0.032          | 19(C) | -0.024 | -0.022 | 0.0467 | 0.0707         | -0.001         | 0.0345         |
| 20(C)  | -0.020 | -0.045 | 0.0238 | 0.0447         | 0.0246         | 0.0347         | 20(C) | -0.023 | -0.034 | 0.014  | 0.0378         | 0.0109         | 0.0244         |
| 21(C)  | -0.032 | -0.057 | 0.0152 | 0.0479         | 0.0252         | 0.0365         | 21(C) | -0.036 | -0.053 | 0.015  | 0.0516         | 0.017          | 0.0343         |
| 22(C)  | -0.037 | -0.057 | -0.002 | 0.035          | 0.0192         | 0.0271         | 22(C) | -0.050 | -0.063 | -0.001 | 0.0491         | 0.0128         | 0.0309         |
| 24(C)  | -0.043 | -0.065 | -0.001 | 0.0424         | 0.0222         | 0.0323         | 24(C) | -0.070 | -0.082 | -0.015 | 0.0544         | 0.0127         | 0.0335         |
| 26(C)  | 0.0292 | -0.008 | 0.0961 | 0.0669         | 0.0373         | 0.0521         | 26(C) | 0.0824 | 0.0585 | 0.1505 | 0.0681         | 0.0239         | 0.046          |
| 29(Cl) | -0.056 | -0.116 | 0.0779 | 0.1345         | 0.0603         | 0.0974         | 29(O) | -0.125 | -0.139 | -0.050 | 0.0751         | 0.014          | 0.0445         |
|        |        |        |        |                |                |                | 30(C) | 0.0046 | -0.001 | 0.0253 | 0.0207         | 0.0064         | 0.0135         |

Table 6 Order of the reactive sites on compounds MBTC and FMTC

| MBTC  |        |        |        |                |                |                | FMTC  |        |        |        |                |                |                |
|-------|--------|--------|--------|----------------|----------------|----------------|-------|--------|--------|--------|----------------|----------------|----------------|
| Atoms | q(N)   | q(N+1) | q(N-1) | f <sup>-</sup> | f <sup>+</sup> | f <sup>0</sup> | Atoms | q(N)   | q(N+1) | q(N-1) | f <sup>-</sup> | f <sup>+</sup> | f <sup>0</sup> |
| 1(C)  | -0.046 | -0.115 | -0.057 | 0.105          | 0.0683         | 0.0289         | 1(C)  | -0.044 | -0.091 | 0.0373 | 0.0067         | 0.0479         | 0.0273         |
| 2(C)  | 0.1745 | 0.1433 | 0.1755 | 0.001          | 0.0312         | 0.0161         | 2(C)  | 0.1676 | 0.1445 | 0.1764 | 0.0087         | 0.0231         | 0.0159         |
| 3(C)  | 0.111  | 0.0672 | 0.1118 | 0.0008         | 0.0438         | 0.0223         | 3(C)  | 0.1022 | 0.0623 | 0.1195 | 0.0173         | 0.0399         | 0.0286         |
| 4(C)  | 0.0431 | -0.066 | 0.0534 | 0.0103         | 0.1095         | 0.0599         | 4(C)  | 0.0399 | -0.039 | 0.0545 | 0.0146         | 0.0789         | 0.0467         |
| 8(N)  | -0.044 | -0.060 | -0.036 | 0.0081         | 0.0158         | 0.0119         | 8(N)  | -0.040 | -0.057 | -0.024 | 0.0155         | 0.0168         | 0.0162         |
| 9(N)  | -0.052 | -0.086 | -0.049 | 0.0033         | 0.0338         | 0.0185         | 9(N)  | -0.050 | -0.079 | -0.036 | 0.0136         | 0.0287         | 0.0211         |
| 10(S) | -0.284 | -0.461 | -0.218 | 0.066          | 0.1774         | 0.1217         | 10(S) | -0.272 | -0.433 | -0.074 | 0.1982         | 0.1614         | 0.1798         |
| 11(O) | -0.266 | -0.328 | -0.258 | 0.0082         | 0.0617         | 0.0349         | 11(O) | -0.263 | -0.312 | -0.234 | 0.0292         | 0.0485         | 0.0388         |
| 12(C) | 0.1672 | 0.1367 | 0.1912 | 0.024          | 0.0305         | 0.0272         | 12(C) | 0.1624 | 0.1298 | 0.1822 | 0.0198         | 0.0325         | 0.0262         |
| 13(N) | -0.047 | -0.050 | 0.0326 | 0.0798         | 0.003          | 0.0414         | 13(N) | -0.038 | -0.047 | 0.0136 | 0.052          | 0.0091         | 0.0306         |
| 15(N) | -0.081 | -0.097 | -0.008 | 0.0724         | 0.016          | 0.0442         | 15(N) | -0.084 | -0.123 | -0.031 | 0.0534         | 0.0392         | 0.0463         |
| 16(O) | -0.266 | -0.323 | -0.197 | 0.0691         | 0.057          | 0.0631         | 16(O) | -0.26  | -0.317 | -0.206 | 0.0532         | 0.0578         | 0.0555         |
| 17(C) | 0.0268 | -0.026 | 0.0743 | 0.0475         | 0.0527         | 0.0501         | 17(C) | 0.0161 | -0.048 | 0.0535 | 0.0375         | 0.0647         | 0.0511         |
| 19(C) | -0.014 | -0.016 | 0.0454 | 0.06           | 0.0015         | 0.0308         | 19(C) | 0.0477 | 0.0342 | 0.1029 | 0.0552         | 0.0135         | 0.0344         |
| 20(C) | -0.028 | -0.042 | 0.0177 | 0.0462         | 0.0144         | 0.0303         | 20(C) | -0.053 | -0.1   | 0.0093 | 0.0632         | 0.0461         | 0.0546         |
| 21(C) | -0.039 | -0.058 | 0.0121 | 0.052          | 0.0189         | 0.0354         | 21(O) | -0.08  | -0.103 | -0.050 | 0.0296         | 0.0233         | 0.0264         |
| 22(C) | -0.040 | -0.054 | -0.001 | 0.0384         | 0.014          | 0.0262         | 22(C) | -0.066 | -0.095 | -0.012 | 0.0545         | 0.0289         | 0.0417         |
| 24(C) | -0.047 | -0.062 | -0.000 | 0.0465         | 0.0154         | 0.031          | 24(C) | 0.0277 | -0.023 | 0.1192 | 0.0916         | 0.0511         | 0.0713         |
| 26(C) | 0.0135 | -0.015 | 0.0934 | 0.0799         | 0.0286         | 0.0542         |       |        |        |        |                |                |                |
| 29(C) | -0.082 | -0.090 | -0.059 | 0.0225         | 0.0087         | 0.0156         |       |        |        |        |                |                |                |

### 3.5 Molecular electrostatic potential (MESP)

The electron density is an incredibly significant factor for investigating the reactivity of electrophilic (E) and nucleophilic (Nu) sites and the interactions of hydrogen bond [30], as well as this density, is related to the molecular electrostatic potential (MESP). Therefore, for predicting this reactivity of Nu and E sites attacks for all studied MSs, we obtained the MESP of these MSs usage the CAM-B3LYP /6-311G++(2d, 2p) level of theory. The numerous colors (red, blue, and green) at the MESP surface indicate different values of the ESP as the regions of highest negative, highest positive, and zero ESP respectively. The negative sites at MESP (red) refer to E reactivity, and the positive sites (blue) refer to Nu reactivity, and

green represent regions of zero potential (See Fig. 5). As presented in Fig. 5, the maximum positive region for all studied MSs is localized on a hydrogen atom is linked to nitrogen atom (N-H) which indicates that this area is an attracting site of electrons. On the other side, the maximum negative region for all studied MSs is localized on the carbonyl group (C=O) which indicates this area is a donating site of electrons.

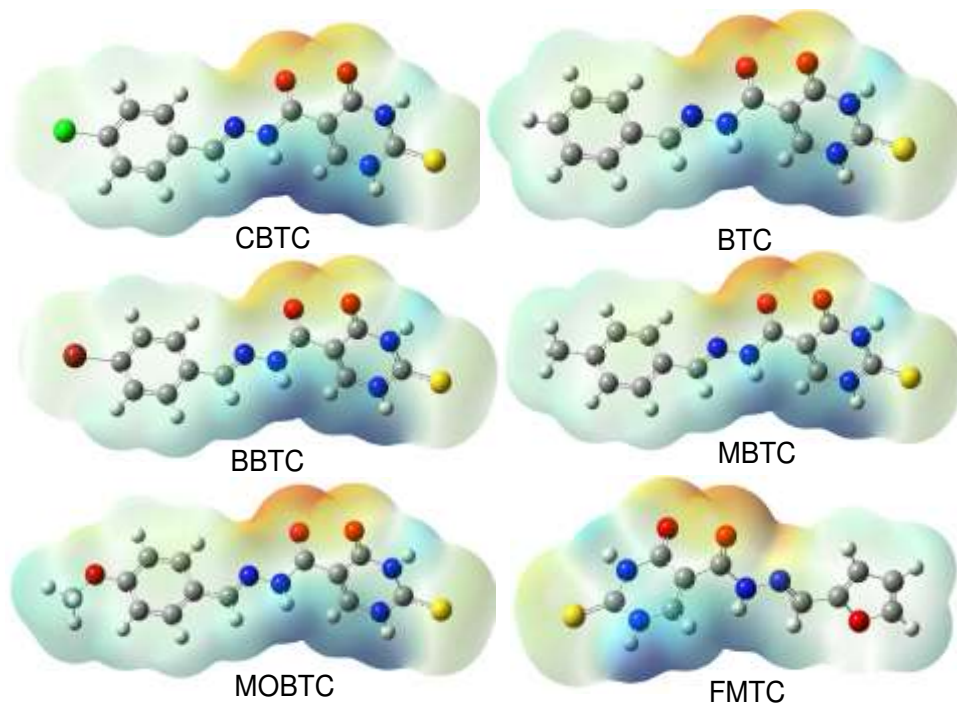


Fig. 5 Calculated MESP on the molecular surfaces of studied compounds. CAM-B3LYP functional and 6-311G ++ (2d, 2p) basis set.

### 3.6 Application

Fig. 6 exhibits the MO energy levels of the six MSs BTC, CBTC, BBTC, MBTC, MOBTC, and FMTC in a gaseous state at DFT/CAM-B3LYB/6-31G++(2d, 2p) level of theory. For the MSs understudy, the HOMO energy is lower than the energy of I<sup>-</sup>/I<sub>2</sub> (-4.85 eV). This indicates that all studied MSs (BTC, CBTC, BBTC, MBTC, MOBTC, and FMTC) can more easily recover electrons

from electrolytes ( $I_3^-$ ). In addition, the LUMO energy of the six studied molecules (BTC, CBTC, BBTC, MBTC, MOBTC, and FMTC) is higher than the conduction band (CB) energy of semiconductor  $TiO_2$  ( $-4.00$  eV) as shown in Fig. 6. Indicating, the electrons can be successfully transferred into  $TiO_2$  from the excited state of all studied dyes. Consequently, all studied MSs dyes may be good candidates for application in PV devices.

The conversion efficiency ( $\eta$ ) of sunlight to electrical energy in SC devices is determined by the short-circuit current density ( $J_{sc}$ ), the open-circuit PV ( $V_{oc}$ ), the fill factor (FF), and incident solar power ( $P_{inc}$ ). The  $\eta$  can be estimated via utilizing Eq. (1) [31]:

$$\eta = \frac{J_{sc} V_{oc} FF}{P_{inc}} \quad (1)$$

from the formula, it can be seen that high  $V_{oc}$  and  $J_{sc}$  are the basis for producing photoelectric conversion efficiency. The maximum value for  $V_{oc}$  is a significant PV parameter that can be obtained computationally via utilizing the difference among the HOMO of dye and the LUMO of the electron acceptor (conduction band of  $TiO_2$ ). The computational value of  $V_{oc}$  have been calculated via utilizing Eq. (2) [27,32]:

$$V_{oc} = |E_{HOMO}^{donor}| - |E_{LUMO}^{acceptor}| - 0.3 \quad (2)$$

However, in DSSCs,  $V_{oc}$  can be obtained as the different energy among LUMO of the dye and conduction band (CB) of the semiconductor [27,32].

$$TiO_2 (E_{CB} = -4.0 \text{ eV}): V_{oc} = |E_{LUMO}^{dye}| - E_{CB} \quad (3)$$

The theoretically calculated value of  $V_{oc}$  for all studied MSs is presented in Table 7. The range value of  $V_{oc}$  is 1.814 to 3.214 eV for  $TiO_2$ . These values are positive; indicating the electron transfer will be easy from all studied MSs to  $TiO_2$ . Furthermore, these values are sufficient to give the best efficient electron injection.

Moreover, those studied MSs can be utilized as sensitizers being of the electron injection process from the excited dye to the conduction band of TiO<sub>2</sub>.

Another parameter denoted ( $\alpha$ ) calculated via the difference between the LUMO energy levels of the studied dyes and the LUMO energy level of PCBM (-3.2eV) [33]. The value can be obtained via using Eq. (4):

$$\alpha = |E_{LUMO}^{acceptor}| - |E_{LUMO}^{donor}| \quad (4)$$

The light-harvesting efficiency (LHE) is obtained using the following equation ( $LHE = 1 - 10^{-f}$ ) [33], where  $f$  is the oscillator strength of the dye MS; the calculated LHE is presented in Table 7. The  $f$  values for all studied MSs were calculated using the TD-DFT/CAM-B3LYP/6-3111G++(2d, 2p) method.

As presented in Table 7, the obtained values of  $\alpha$  were in the range of (1.014-2.414 eV). Indicating, that all LUMO MO level for all studied MSs is placed higher than the LUMO MO level of PCBM [33]. So, these studied compounds can be utilized as sensitizers being of the electron injection process from the excited dye to the conduction band of PCBM. Since the value of LHE increase in the following order as shown in Table 7; FMTC < BTC < MBTC < CBTC = MOBTC < BBTC therefore the best dye that can act as DSSCs is BBTC dye comparable to the rest compounds under study. The LHE value for BTC was 0.856 eV as shown in Table 7. The presence of chloride (Cl<sup>-</sup>), bromide (Br<sup>-</sup>), methyl (CH<sub>3</sub>-), and methoxy (CH<sub>3</sub>-O-) substituents at the para position of the phenyl group in CBTC, BBTC, MBTC, and MOBTC MSs respectively enhance the LHE by the range of (0.078-0.095) eV. This is due to EW properties of Cl<sup>-</sup> and Br<sup>-</sup> and ED properties of CH<sub>3</sub>- and CH<sub>3</sub>-O-. On the other hand, comparable FMTC to BTC, the LHE of FMTC is decreased via 0.22 eV due to the substitution of furan with a phenyl group. The LHE values for BTC, CBTC, BBTC, MBTC, and MOBTC were in the close range (0.856-0.951) indicating that those MSs gave similar photocurrent [34].

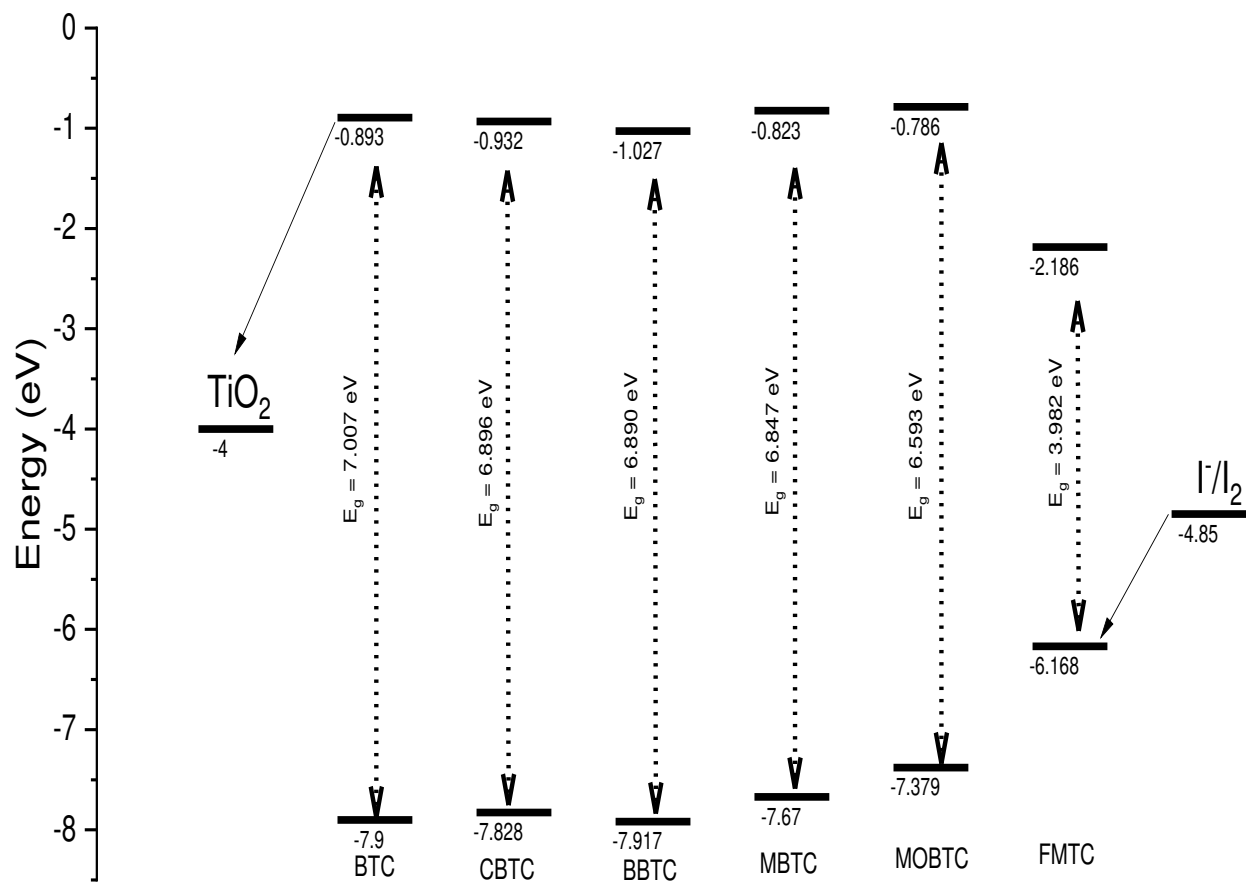


Fig. 6 Frontier molecular orbital energies and energy gaps of  $\text{TiO}_2$ , BTC, CBTC, BBTC, MBTC, MOBTC, FMTC and  $\text{I}^-/\text{I}_2$ .

Table 7 Energy values of  $E_{\text{HOMO}}$ ,  $E_{\text{LUMO}}$ , open circuit voltage ( $V_{\text{oc}}$ ) and light harvesting efficiency (LHE) by eV.

| Compounds | $E_{\text{HOMO}}$ (eV) | $E_{\text{LUMO}}$ (eV) | $V_{\text{oc}}$ (eV) | $\alpha$ (eV) | LHE(ev) |
|-----------|------------------------|------------------------|----------------------|---------------|---------|
| BTC       | -7.900                 | -0.893                 | 3.107                | 2.307         | 0.856   |
| CBTC      | -7.828                 | -0.932                 | 3.068                | 2.268         | 0.944   |
| BBTC      | -7.917                 | -1.027                 | 2.973                | 2.173         | 0.951   |
| MBTC      | -7.670                 | -0.823                 | 3.177                | 2.377         | 0.934   |
| MOBTC     | -7.379                 | -0.786                 | 3.214                | 2.414         | 0.944   |
| FMTC      | -6.168                 | -2.186                 | 1.814                | 1.014         | 0.636   |

## Conclusion

In this paper, the optimized molecular structures, NBO analysis, ESP calculation, Fukui function analysis and DFT calculations of six 1,2,3,4-tetrahydropyrimidine-5-carbohydrazide (BTC, CBTC, BBTC, MBTC, MOBTC and FMTC) were investigated successfully via utilizing DFT/CAM-B3LYP/6-311G++(2d, 2p) method. According to the ground state geometry, we note that all stable conformations are planar. The HOMO/LUMO energy gaps of BTC, CBTC, BBTC, MBTC, MOBTC and FMTC were calculated at DFT/CAM-B3LYP/6-31G++(2d, 2p) level are 7.007, 6.896, 6.890, 6.847, 6.593 and 3.982eV respectively. So, the energy gaps differ slightly and decrease in the following order; FMTC < MOBTC < MBTC < BBTC < CBTC < BTC. Consequently, the calculated values of  $V_{\text{oc}}/\text{TiO}_2$  of our dyes are sufficient for a possible efficient electron injection from the donor to the acceptor.

**Code availability** N/A

**Author contribution:** **Mahmoud A.S. Sakr:** Data curation, Methodology, Software, Supervision. **Farag F. Sherbiny:** Writing - review & editing. **Abd-Allah Sh. El-Etrawy:** Visualization, Investigation.

**Funding:** This work was supported by Misr University for Science and Technology (Center of Basic Science).

**Data availability:** All data generated or analyzed during this study are included in this published article.

## **Declarations**

**Conflict of interest:** The authors declare no competing interests

## **References**

- [1] Narang R, Narasimhan B, Sharma S. A review on biological activities and chemical synthesis of hydrazide derivatives. *Curr Med Chem* 2012;19:569–612.
- [2] Rose MG, Farrell MP, Schmitz JC. Thymidylate synthase: a critical target for cancer chemotherapy. *Clin Colorectal Cancer* 2002;1:220–9.
- [3] Palla G, Predieri G, Domiano P, Vignali C, Turner W. Conformational behaviour and E/Z isomerization of N-acyl and N-arylohydrazones. *Tetrahedron* 1986;42:3649–54.
- [4] Dimmock JR, Vashishtha SC, Stables JP. Anticonvulsant properties of various acetylhydrazones, oxamoylhydrazones and semicarbazones derived from aromatic and unsaturated carbonyl compounds. *Eur J Med Chem* 2000;35:241–8.
- [5] Lima PC, Lima LM, Da Silva KCM, Léda PHO, Miranda A. LP; Fraga, CAM; Barreiro, EJ. *Eur J Med Chem* 2000;35:187.
- [6] Silva GA, Costa LMM, Brito FCF, Miranda ALP, Barreiro EJ, Fraga CAM. New class of potent antinociceptive and antiplatelet 10H-phenothiazine-1-acylhydrazone derivatives. *Bioorg Med Chem* 2004;12:3149–58.
- [7] Asim Kaplancikli Z, Dilek Altintop M, Ozdemir A, Turan-Zitouni G, I Khan S, Tabanca N. Synthesis and biological evaluation of some hydrazone

- derivatives as anti-inflammatory agents. *Lett Drug Des Discov* 2012;9:310–5.
- [8] Fattorusso C, Campiani G, Kukreja G, Persico M, Butini S, Romano MP, et al. Design, synthesis, and structure–activity relationship studies of 4-quinolinyl- and 9-acridinylhydrazones as potent antimalarial agents. *J Med Chem* 2008;51:1333–43.
- [9] Mariotti N, Bonomo M, Fagiolari L, Barbero N, Gerbaldi C, Bella F, et al. Recent advances in eco-friendly and cost-effective materials towards sustainable dye-sensitized solar cells. *Green Chem* 2020;22:7168–218.
- [10] Vlachopoulos N, Hagfeldt A, Benesperi I, Freitag M, Hashmi G, Jia G, et al. New approaches in component design for dye-sensitized solar cells. *Sustain Energy Fuels* 2021;5:367–83.
- [11] Kokkonen M, Talebi P, Zhou J, Asgari S, Soomro SA, Elsehrawy F, et al. Advanced research trends in dye-sensitized solar cells. *J Mater Chem A* 2021.
- [12] Chalkias DA, Loizos DD, Papanicolaou GC. Evaluation and prediction of dye-sensitized solar cells stability under different accelerated ageing conditions. *Sol Energy* 2020;207:841–50.
- [13] Ansari AA, Nazeeruddin MK, Tavakoli MM. Organic-inorganic upconversion nanoparticles hybrid in dye-sensitized solar cells. *Coord Chem Rev* 2021;436:213805.
- [14] Liao C, Zeng K, Wu H, Zeng Q, Tang H, Wang L, et al. Conjugating pillararene dye in dye-sensitized solar cells. *Cell Reports Phys Sci* 2021;2:100326.
- [15] Lee M-W, Kim J-Y, Lee H-G, Cha HG, Lee D-H, Ko MJ. Effects of structure and electronic properties of D- $\pi$ -A organic dyes on photovoltaic performance of dye-sensitized solar cells. *J Energy Chem* 2021;54:208–16.
- [16] Zakutayev A, Major JD, Hao X, Walsh A, Tang J, Todorov TK, et al. Emerging inorganic solar cell efficiency tables (version 2). *J Phys Energy* 2021;3:32003.
- [17] Grätzel M. Recent advances in sensitized mesoscopic solar cells. *Acc Chem Res* 2009;42:1788–98.
- [18] Li G, Shrotriya V, Huang J, Yao Y, Moriarty T, Emery K, et al. High-

- efficiency solution processable polymer photovoltaic cells by self-organization of polymer blends. *Mater. Sustain. Energy A Collect. Peer-Reviewed Res. Rev. Artic. from Nat. Publ. Gr., World Scientific*; 2011, p. 80–4.
- [19] Yang W, Cao D, Zhang H, Yin X, Liao X, Huang J, et al. Dye-sensitized solar cells based on (DĀpĀA) 3L2 phenothiazine dyes containing auxiliary donors and flexible linkers with different length of carbon chain. *Electrochim Acta* 1732;283:2018.
- [20] Ardo S, Meyer GJ. Photodriven heterogeneous charge transfer with transition-metal compounds anchored to TiO<sub>2</sub> semiconductor surfaces. *Chem Soc Rev* 2009;38:115–64.
- [21] O’regan B, Grätzel M. A low-cost, high-efficiency solar cell based on dye-sensitized colloidal TiO<sub>2</sub> films. *Nature* 1991;353:737–40.
- [22] El-Etrawy A-AS, Sherbiny FF. Design, synthesis, biological evaluation and molecular modeling investigation of new N’-(2-Thiouracil-5-oyl) hydrazone derivatives as potential anti-breast cancer and anti-bacterial agents. *J Mol Struct* 2021;1232:129993.
- [23] Horiuchi T, Miura H, Sumioka K, Uchida S. High efficiency of dye-sensitized solar cells based on metal-free indoline dyes. *J Am Chem Soc* 2004;126:12218–9.
- [24] Jia C, Wan Z, Zhang J, Li Z, Yao X, Shi Y. Theoretical study of carbazole–triphenylamine-based dyes for dye-sensitized solar cells. *Spectrochim Acta Part A Mol Biomol Spectrosc* 2012;86:387–91.
- [25] Luo-Xin W, Yong L, Xin-Lin T, Song-Nian L, Mao-Gong W. Effect of H<sup>+</sup> and NH<sub>4</sub><sup>+</sup> on the N-NO<sub>2</sub> bond dissociation energy of HMX. *Acta Physico-Chimica Sin* 2007;23:1560–4.
- [26] Lu T, Chen F. Multiwfn: a multifunctional wavefunction analyzer. *J Comput Chem* 2012;33:580–92.
- [27] Bourass M, Benjelloun AT, Benzakour M, Mcharfi M, Hamidi M, Bouzzine SM, et al. DFT and TD-DFT calculation of new thienopyrazine-based small molecules for organic solar cells. *Chem Cent J* 2016;10:1–11.
- [28] El-Daly SA, Alamry KA. Spectroscopic Investigation and Photophysics of a D- $\pi$ -A- $\pi$ -D Type Styryl Pyrazine Derivative. *J Fluoresc* 2016;26:163–76.

- [29] Halim SA, Khalil AK. TD-DFT calculations, NBO analysis and electronic absorption spectra of some thiazolo [3, 2-a] pyridine derivatives. *J Mol Struct* 2017;1147:651–67.
- [30] Bendjeddou A, Abbaz T, Gouasmia AK, Villemin D. Molecular structure, HOMO-LUMO, MEP and Fukui function analysis of some TTF-donor substituted molecules using DFT (B3LYP) calculations. *Int Res J Pure Appl Chem* 2016:1–9.
- [31] Ghosh NN, Habib M, Pramanik A, Sarkar P, Pal S. Molecular engineering of anchoring groups for designing efficient triazatruxene-based organic dye-sensitized solar cells. *New J Chem* 2019;43:6480–91.
- [32] Bourass M, Benjelloun AT, Benzakour M, Mcharfi M, Jhilal F, Serein-Spirau F, et al. DFT/TD-DFT characterization of conjugational electronic structures and spectral properties of materials based on thieno [3, 2-b][1] benzothiophene for organic photovoltaic and solar cell applications. *J Saudi Chem Soc* 2017;21:563–74.
- [33] Bouachrine M. New organic dyes based on phenylenevinylene for solar cells: DFT and TD-DFT investigation n.d.
- [34] Ogunyemi BT, Oyeneyin OE, Esan OT, Adejoro IA. Computational modelling and characterisation of phosphole adopted in triphenyl amine photosensitisers for solar cell applications. *Results Chem* 2020;2:100069.